Effects of AlN film thickness and operating frequency on sensing output of CO_2 pyroelectric-based non-dispersive infrared gas sensor

Doris Keh Ting Ng*[a], Kristel Pei Xuan Wee[a], Md Hazwani Khairy Md Husni[a], Landobasa Tobing[a], Wing Wai Chung[a], Isaac Siyuan Ling[a], Norhanani Jaafar[a], Jia Sheng Goh[a], Linfang Xu[a], Weiguo Chen[a], Qingxin Zhang[a]
[a]Institute of Microelectronics (IME), Agency for Science, Technology and Research (A*STAR), 2 Fusionopolis Way, Innovis #08-02, Singapore 138634, Republic of Singapore

ABSTRACT

CMOS compatible AlN-based pyroelectric detectors of different thicknesses (500 nm and 1 μm respectively) are examined by measuring their responses to different concentrations of CO_2 gas in an NDIR gas sensing system. We note up to ~55% improvement in signal when AlN thickness reduces from 1 μm to 500 nm. In addition, we design our AlN-based pyroelectric detectors similar to 2 capacitors connected in series and 4 capacitors connected in series while keeping the total pyroelectric sensing layer constant. CO_2 sensing responses of both designs with AlN thicknesses of 500 nm and 1 μm are measured in the NDIR gas sensing system and the 2-capacitor design with 500 nm thick AlN in general gives a more sensitive response. The LOD for CO_2 sensing when using this detector is extracted based on Beer-Lambert law and we obtain an LOD of ~53ppm. As pyroelectric detectors are known to operate at lower frequencies (~tens of hertz), we also operate the detectors at different modulating frequencies (7 Hz, 11 Hz and 17.4 Hz) and observe their effects on the gas sensing signal. Comparing the 4 different detectors in NDIR gas sensing, the AlN-based pyroelectric detector with 500 nm thick AlN and of 2-capacitor design presents the best performance in CO_2 gas sensing. This work shows effects of AlN film thickness change and variation in operating frequency on pyroelectric-based NDIR CO_2 gas sensing. The results will provide more understanding on characteristics of AlN-based pyroelectric detectors and their behaviours in NDIR gas sensing.

Keywords: greenhouse gases, CO_2 gas sensor, carbon dioxide, pyroelectric detector, aluminum nitride, CMOS compatible, non-dispersive infrared, modulating frequency

1. INTRODUCTION

Carbon dioxide (CO_2) is a greenhouse gas. Increasing levels of CO_2 concentration in the environment not only impact climate, but will also affect health, commonly known as sick building syndrome (SBS) where symptoms such as headaches, drowsiness and difficulty in concentrating appear when CO_2 gas levels increase to 1000 ppm and above.[1-2] A CO_2 gas sensor will allow one to monitor the level of CO_2 concentration in the air. Non-dispersive infrared (NDIR),[3-4] a technique which makes use of gas absorption at mid- infrared (IR) molecular fingerprint wavelength region is commonly used for CO_2 gas sensing. As CO_2 gas has a strong isolated absorption peak at ~4.26 μm, this method of sensing is highly selective and non-poisoning.[5-6]

NDIR gas sensors usually consist of a source, a detector and a gas channel in between.[4,7-8] It leverages on the interaction between source-detector optical pathlength and gas absorption of light at particular wavelengths to enable gas sensing. Pyroelectric detectors are uncooled thermal detectors that have been demonstrated in applications such as fire alarms, thermal imaging,[9] contactless button sensing,[10] thermal conductivity gas sensing[11] and NDIR gas sensing.[3-4,8] In particular, complementary metal-oxide-semiconductor (CMOS) compatible aluminum nitride (AlN) -based pyroelectric detector and its doped counterpart scandium aluminum nitride (ScAlN) –based pyroelectric detector are gaining interest in the research community[12-16] as they could be deposited across full wafers, making them scalable across 8-inch and 12-inch wafers, bringing promise towards large scale manufacturability. Their low deposition temperature of ~200°C (< 500°C)[13-14,17-18] also opens up the possibility of integration with CMOS electronics. On top of that, these materials have multifaceted properties, from gas sensing and piezoelectric[19] to photonics,[20] which could potentially allow for ease of integration for a multi-functional device.

*doris_ng@ime.a-star.edu.sg; phone 65 6826 6111; www.a-star.edu.sg/ime

In this work, we examine AlN-based pyroelectric detectors in NDIR CO_2 gas sensing. AlN of 2 different thicknesses (500 nm and 1 µm) and 2 different designs are fabricated and tested for their CO_2 gas sensing response. We note that a thinner pyroelectric sensing layer (AlN = 500 nm) exhibits a higher output signal compared to a thicker pyroelectric sensing layer (AlN = 1 µm), with higher output signal up to 55% more. The limit of detection (LOD) is calculated from the gas sensing response plots and LODs obtained varies ~53 ppm to ~145 ppm from 4 different AlN-based pyroelectric detectors.

In addition, gas sensing outputs of these AlN-based pyroelectric detectors are examined at different frequencies from 6 Hz - 40 Hz to examine their output trend with modulating frequency. We note, in general, optimal operating frequency for maximum gas sensing response to be ~17.4 Hz when using AlN-based pyroelectric detector with 500 nm AlN thickness and ~11 Hz when using AlN-based pyroelectric detector with 1 µm AlN thickness. The results obtained will provide more insights to behaviors of AlN-based pyroelectric detectors with different pyroelectric sensing layer thicknesses and designs in an NDIR gas sensing system.

2. EXPERIMENTAL

Figure 1a shows a schematic of an NDIR CO_2 gas sensor formed by putting together a thermal emitter, a 10 cm aluminum (Al) channel and a pyroelectric detector. More details of this NDIR gas sensor formation can be found in literature.[21] Optical narrow bandpass filters with centre wavelength (λ) at ~4.26 µm are inserted after the thermal emitter and before the pyroelectric detector to allow CO_2 absorption wavelength (λ~4.26 µm) to pass through. AlN-based pyroelectric detector is used in this work and a cross-sectional zoom-in (Fig. 1b) shows AlN sensing layer sandwiched between bottom electrode molybdenum (Mo) and top electrode titanium nitride (TiN). Beneath the bottom electrode Mo is a thermal isolating layer of SiO_2 followed by air cavity. The final form of the detector stack will be in membrane form allowing more thermal energy to be retained within the pyroelectric sensing layer which will then later be converted to output electrical signal. On top of the top electrode TiN is an absorber stack consisting of silicon dioxide (SiO_2) and silicon nitride (SiN) layers to allow more mid-IR absorption onto the detector. A previous study[12] has revealed that AlN-based pyroelectric detector stack with a thinner 500 nm AlN sensing layer has shown higher absorption at λ~4.26 µm compared to a thicker 1 µm AlN sensing layer measured by a Fourier Transform Infrared (FTIR) system. This CO_2 gas sensor is tested with AlN-based pyroelectric detectors with 2 different AlN thicknesses – 500 nm and 1 µm. As pyroelectric detectors appear like capacitors with accumulation of charges on the top and bottom electrodes upon sensing temperature fluctuations, we design the pyroelectric detectors similar to 2 capacitors connected in series and 4 capacitors connected in series as shown in Fig. 1c, keeping the total accumulated AlN sensing area of each detector constant at 0.25 mm^2.

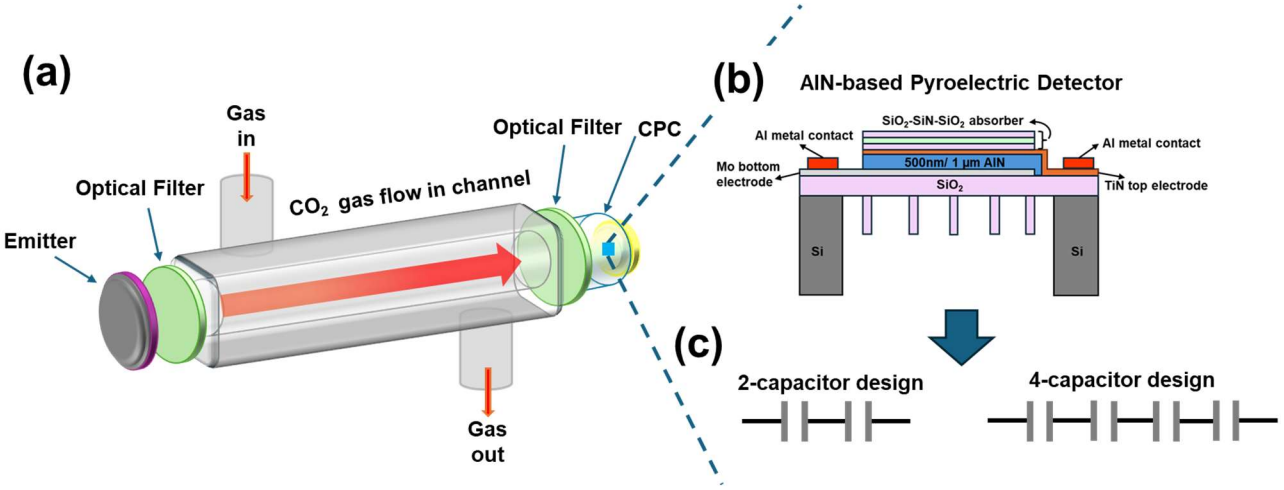

Figure 1. (a) Schematic of the NDIR CO_2 gas sensor formed by putting the respective components together. (b) Zoom-in cross-sectional view of the detector which is AlN-based pyroelectric detector with AlN thickness of 500 nm or 1 µm. (c) The AlN-based pyroelectric detectors tested in this NDIR CO_2 gas sensor come in 2 designs (2-capacitor connected in series and 4-capacitor connected in series).

3. RESULTS AND DISCUSSION

CO_2 gas testing of the NDIR CO_2 gas sensor is conducted using AlN-based pyroelectric detectors of different designs, cycled between different concentration of CO_2 (300 ppm – 5000 ppm) and nitrogen (N_2) used as the reference gas. The modulating frequency of the emitter is set at 17.4 Hz. Figure 2 shows the CO_2 gas sensing response using different AlN-based pyroelectric detectors. Figure 2a and 2b show CO_2 gas sensing responses using detectors with 2-capacitor design while Fig. 2c and 2d show that using 4-capacitor design. We note that for both designs, the detector with a thinner (500 nm) AlN pyroelectric sensing layer gives a higher output signal voltage compared to the detector with thicker (1 µm) AlN. When N_2 passes through the gas channel, Fig. 2a measures a higher voltage of ~560 µV compared to Fig. 2b which measures a voltage of ~395 µV while Fig. 2c shows a higher voltage of ~324 µV compared to Fig. 2d of ~209 µV. In addition, when CO_2 gas passes through the gas channel, the voltage drop from N_2 to CO_2 is larger for the pyroelectric detector with 500 nm thick AlN for both designs. The voltage drop for Fig. 2a (when AlN is 500 nm thick) from N_2 to 5000 ppm CO_2 gas is ~212 µV while that for Fig. 2b (when AlN is 1 µm thick) is ~145 µV. This is around 46% increase when the AlN thickness is halved. With 500 nm thick AlN exhibiting a higher voltage when N_2 gas passes through and a greater drop in voltage from N_2 to CO_2 when CO_2 gas enters the gas channel, it signifies that AlN-based pyroelectric detector with a thinner pyroelectric sensing layer performs better and hence could allow for a LOD.

Figure 2e depicts the voltage increase when N_2 passes through the gas channel for both designs. The 2-capacitor design gives a higher absolute voltage and increases ~42% when AlN layer thickness decrease from 1 µm to 500 nm. Similar trend is observed for 4-capacitor design and the increase is ~55% when AlN thickness decreases.

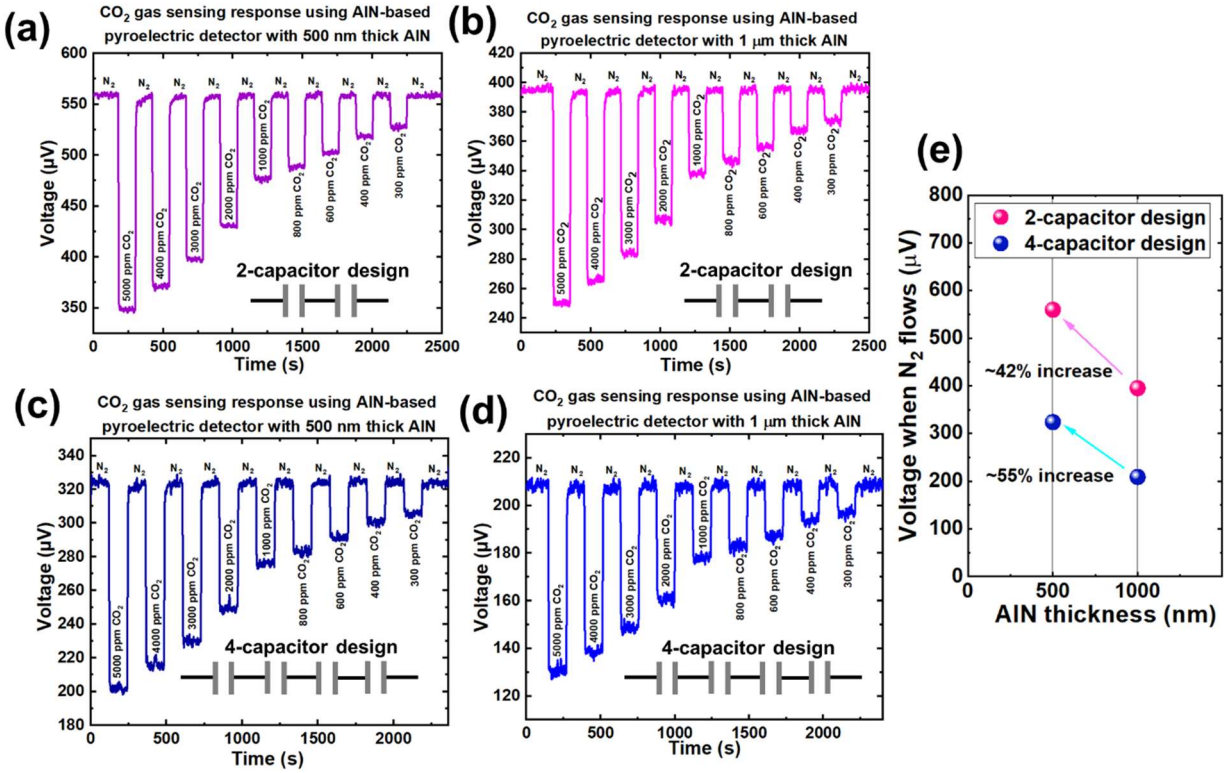

Figure 2. Gas sensing response of CO_2 gas over concentration range from 300 ppm – 5000 ppm cycled between N_2 and different concentrations of CO_2 using AlN-based pyroelectric detector with (a) 2-capacitor design with AlN thickness = 500 nm, (b) 2-capacitor design with AlN thickness = 1 µm, (c) 4-capacitor design with AlN thickness = 500 nm and (d) 4-capacitor design with AlN thickness = 1 µm. (e) Output voltages from the 4 pyroelectric detectors when N_2 flows through the gas channel.

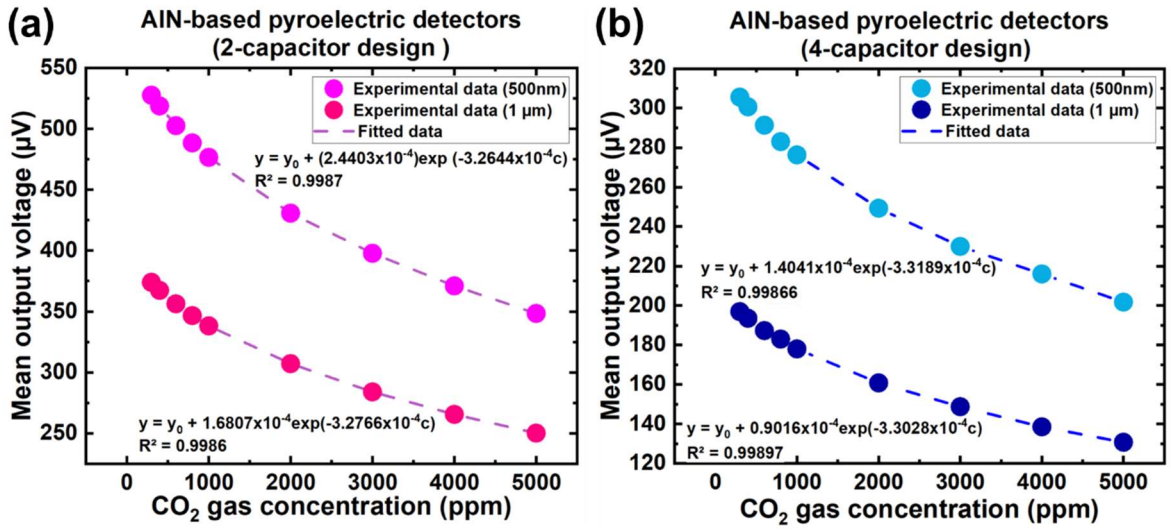

Figure 3. CO_2 gas sensing data fitted based on Beer-Lambert law when (a) 2-capacitor design and (b) 4-capacitor design AlN-based pyroelectric detectors with AlN thicknesses at 500 nm and 1 μm are used in the NDIR gas sensor.

The mean output voltage at respective CO_2 gas concentration (Fig. 3) is then fitted based on Beer-Lambert law[22] using the following equation:

$$y = y_0 + Aexp(-\varepsilon Lc), \quad (1)$$

where A is a prefactor, ε is the molar absorptivity, L is the length of the gas channel and c is the gas concentration. Figure 3a and 3b show the graphical plots when AlN-based pyroelectric detectors with 2-capacitor design and 4-capacitor design respectively are used in the NDIR gas sensor. The LOD is then defined as $LOD = \frac{3.3\sigma}{S}$ [23], where σ is the standard deviation of the output voltage at each gas concentration which can also be considered as the detector noise, S is the slope of the graph at very small gas concentration, defined as

$$S(c \to 0) \equiv dy/dc = -A\varepsilon L \exp(-\varepsilon Lc) = -A\varepsilon L. \quad (2)$$

As presented in Fig. 3, when the experimental data is fitted with Eq (1), the detector with 2-capacitor design and 500 nm AlN thickness returns A = 2.4403x10^{-4} and εL = 3.2644x10^{-4} ppm^{-1}, while the detector with 4-capacitor design and 500nm thickness returns A = 1.4041x10^{-4} and εL = 3.3189x10^{-4} ppm^{-1}. Whereas A = 1.6807 x10^{-4} and εL = 3.2766 x10^{-4} ppm^{-1} when AlN thickness is 1 μm in the 2-capacitor design and A = 0.9016x10^{-4} and εL = 3.3028x10^{-4} ppm^{-1} when AlN thickness is 1 μm in the 4-capacitor design.

LOD extracted varies from 54 ppm – 145 ppm depending on the pyroelectric detector used in the gas sensor. The lowest LOD obtained is ~54 ppm when AlN-based pyroelectric detector with 2-capacitor design, 500 nm thick AlN is used. This is followed by 2-capacitor design with thicker AlN (1 μm) where LOD is ~81 ppm. The highest LOD extracted is ~145 ppm, from the 4-capacitor design AlN-based pyroelectric detector with 1 μm thick AlN. 4-capacitor design with 500 nm thick AlN presents an LOD of ~105 ppm.

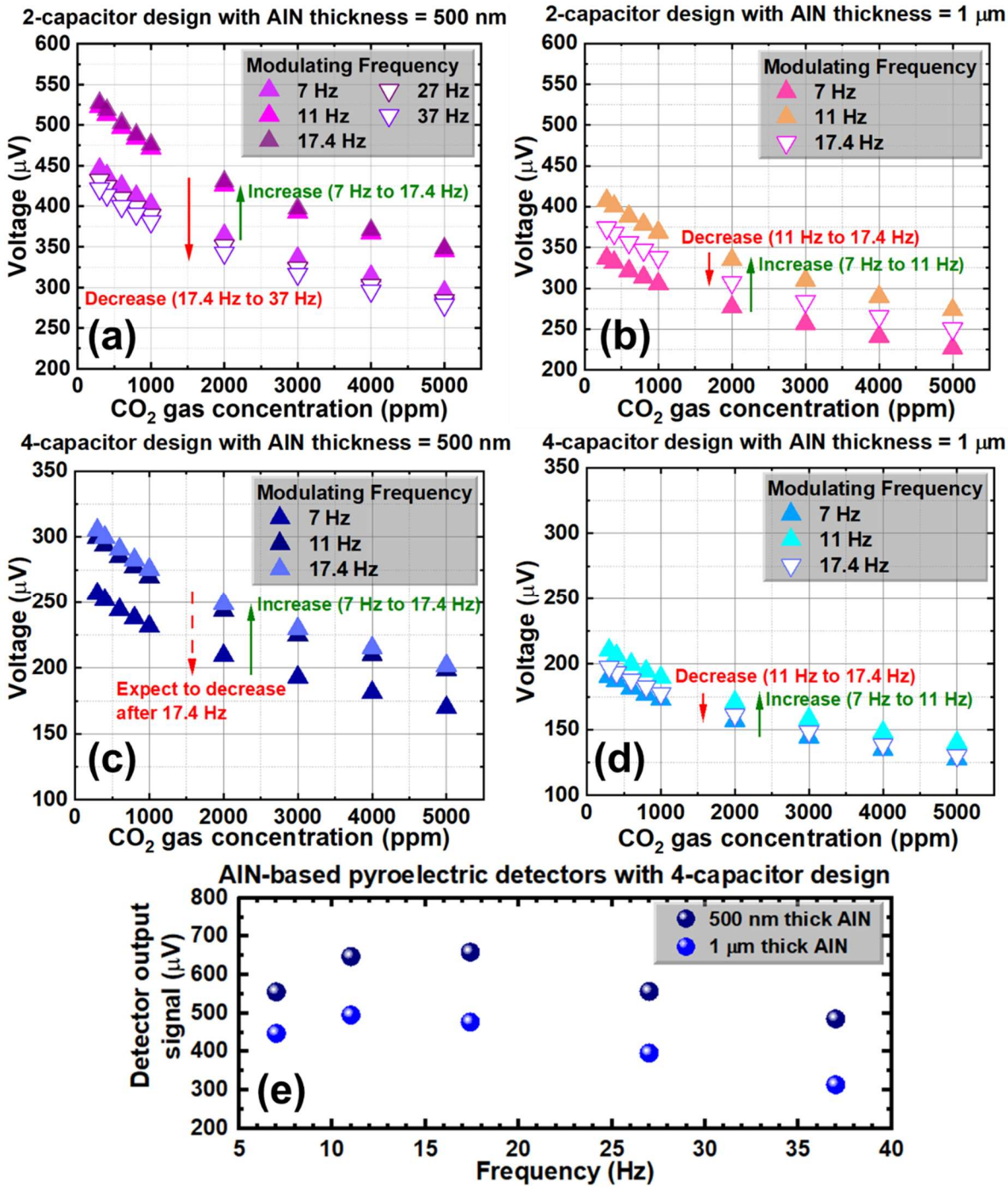

Figure 4. Detector output voltage at different CO_2 gas concentrations over different emitter modulating frequencies for (a) 2-capacitor design with AlN thickness = 500 nm, (b) 2-capacitor design with AlN thickness = 1 μm, (c) 4-capacitor design with AlN thickness = 500 nm, (d) 4-capacitor design with AlN thickness = 1 μm. (d) Trends of detector output signal measured across different frequencies from 5-40 Hz for 500 nm and 1 μm AlN-based pyroelectric detector with 4-capacitor design.

Figure 4 shows the trend of output voltage measured at different CO_2 gas concentrations with AlN-based pyroelectric detectors of different AlN thicknesses (500 nm and 1 μm) and also at different modulating frequencies. As seen earlier from Fig. 2, the output voltage decreases with increasing CO_2 gas concentration. In Fig. 4a-4d, we further note the trend where output voltage changes according to different modulating frequencies. Figure 4a shows the voltage plot with different CO_2 gas concentration for a 2-capacitor design AlN-based pyroelectric detector with AlN sensing thickness of

500 nm. The measurements recorded show an increase in output voltage as frequency increases from 7 Hz to 17.4 Hz but starts to drop as the frequency continues to increase to 27 Hz and 37 Hz. There is an increase of ~18.3 % from frequency of 7 Hz to 17.4 Hz, and a drop of ~20.4% from 17.4 Hz to 37 Hz. It is also worthwhile to note that the output voltage increase slows down from 11 Hz to 17.4 Hz, with voltage increase of ~1.1% (from 11 Hz to 17.4 Hz) compared to ~17% (from 7 Hz to 11 Hz). Similarly, voltage drop slows down as the frequency increases with a drop ~18.4% (from 17.4 Hz to 27 Hz) to ~2.5% (from 27 Hz to 37 Hz). When the pyroelectric detector with 2-capacitor design and thicker AlN (1 µm) is used, output voltage increases from 7 Hz to 11 Hz and starts to drop from 11 Hz to 17.4 Hz as seen in Fig. 4b. We then move on to measure the output voltage with different CO_2 gas concentrations for 4-capacitor design pyroelectric detectors with AlN thicknesses of 500 nm and 1 µm respectively (Fig. 4c and Fig. 4d). Figure 4c exhibits output voltage increase as the frequency increases from 7 Hz to 17.4 Hz, but this increase slows down from 11 Hz to 17.4 Hz. Similar to what we observe from Fig. 4a, we would expect the output voltage to start decreasing as the frequency increases further after 17.4 Hz. In Fig. 4d, the increase from 7 Hz to 11 Hz is ~9.1% which is the lowest among all 4 AlN-based pyroelectric detectors. Output voltage starts to drop after 11 Hz and gives a low drop of ~5.8% from 11 Hz to 17.4 Hz. For 4-capacitor design, the detector output signals are further examined at different frequencies from 5 Hz to 40 Hz in a setup using a shorter gas channel. Consistent with Fig. 4c and 4d, Fig. 4e shows that the detector output signal increases first, then decrease as the modulating frequency increases. In general, AlN-based pyroelectric detector with 500 nm thick AlN gives a higher output signal compared to that of 1 µm AlN thickness. When operating the gas sensor using AlN-based pyroelectric detector with 500 nm AlN sensing layer, optimal frequency is ~17.4 Hz. On the other hand, when operating using AlN-based pyroelectric detector with 1 µm AlN sensing layer, optimal frequency is ~11 Hz.

4. CONCLUSION

NDIR CO_2 gas sensor is built using AlN-based pyroelectric detectors and their respective responses to CO_2 gas sensing are examined. The AlN-based pyroelectric detectors are fabricated over 8-inch wafer with AlN pyroelectric sensing layer of 2 different thicknesses – 500 nm and 1 µm. The pyroelectric detectors are also designed as 2 capacitors connected in series and 4 capacitors connected in series while maintaining the total pyroelectric sensing area for each device. CO_2 gas sensing measurements show that the gas sensor with a thinner AlN layer (500 nm) is more sensitive to CO_2 gas sensing, resulting in a greater voltage drop and lower LOD compared to the gas sensor with a thicker AlN layer (1 µm). A pyroelectric detector with 500 nm thick AlN pyroelectric sensing layer gives an output signal up to 55% increase as compared to that with 1 µm thick AlN. We also note that in general, the pyroelectric detector with 2-capacitor design gives a higher output signal compared to the pyroelectric detector with 4-capacitor design. The LODs for the gas sensing tests using each of the 4 AlN-based pyroelectric detectors in the NDIR gas sensor are extracted after fitting the experimental data with Eq (1) based on Beer-Lambert law and the results show that lowest LOD ~ 53 ppm is obtained when using the pyroelectric detector with 2-capacitor design and AlN thickness of 500 nm. The gas sensor with respective AlN-based pyroelectric detectors are further subjected to gas testing at different modulating frequencies to obtain optimal operating frequency for maximum gas sensing output. For the pyroelectric detector with AlN thickness ~ 500 nm, the optimal operating frequency is at ~17.4 Hz, while for the pyroelectric detector with AlN thickness ~ 1 µm, the optimal operating frequency observed is at ~11 Hz. All in all, the results obtained provide insights on the behaviors of AlN-based pyroelectric detectors in NDIR gas sensing and their suitability could then be considered in different use cases.

ACKNOWLEDGEMENTS

We thank Leh Woon Lim for useful discussion. This research is supported by the National Research Foundation, Singapore, and A*STAR (Agency for Science, Technology and Research), Singapore under its Low-Carbon Energy Research (LCER) Funding Initiative (FI) (Award no.: U2102d2012) for fabrication, testing and LCER Phase 2 (Award no.: U2303D4001) for testing.

REFERENCES

[1] Franco, A., Leccese, F., "Measurement of CO_2 concentration for occupancy estimation in educational buildings with energy efficiency purposes," J. Build. Eng. 32, 101714 (2020). https://doi.org/10.1016/j.jobe.2020.101714

[2] Azuma, K., Kagi, N., Yanagi, U., Osawa, H., "Effects of low-level inhalation exposure to carbon dioxide in indoor environments: A short review on human health and psychomotor performance," Environ. Int. 121, 51-56 (2018). https://doi.org/10.1016/j.envint.2018.08.059

[3] Ng, D. K. T., Ho, C. P., Xu, L., Chen, W., Fu, Y. H., Zhang, T., Siow, L. Y., Jaafar, N., Ng, E. J., Gao, Y., Cai, H., Zhang, Q., Lee, L. Y. T., "NDIR CO_2 gas sensing using CMOS compatible MEMS ScAlN-based pyroelectric detector," Sensors and Actuators: B. Chemical, 346, 130437 (2021). https://doi.org/10.1016/j.snb.2021.130437

[4] Ng, D. K. T., Xu, L., Chen, W., Wang, H., Gu, Z., Chia X. X., Fu, Y. H., Jaafar, N., Ho, C. P., Zhang, T., Zhang, Q., Lee, L. Y. T., "Miniaturized CO_2 Gas Sensor using 20% ScAlN-based pyroelectric detector," ACS Sensors, 7, 2345-2357 (2022). https://doi.org/10.1021/acssensors.2c00980

[5] Hummelga˚rd, C., Bryntse, I., Bryzgalov, M., Henning, J., Martin, H., Norén, M., Rödjega˚rd, H., "Low-cost NDIR based sensor platform for sub-ppm gas detection," Urban Climate, 14, 342-350 (2015). https://doi.org/10.1016/j.uclim.2014.09.001

[6] Fu, L., You, S., Li, G., Fan, Z., "Enhancing methane sensing with NDIR technology: Current trends and future prospects," Reviews in Analytical Chemistry, 42 (1), 20230062 (2023). https://doi.org/10.1515/revac-2023-0062

[7] Ng, D. K. T., Ho, C. P., Xu, L., Chen, W., Fu, Y. H., Zhang, T., Siow, L. Y., Jaafar, N., Ng, E. J., Gao, Y., Cai, H., Zhang, Q., Lee, L. Y. T., "CO_2 gas sensing by CMOS-MEMS ScAlN-based pyroelectric detector based on mid-IR absorption," 2021 21st International Conference on Solid-State Sensors, Actuators and Microsystems (Transducers), Orlando, FL, USA, 827-830 (2021). https://doi.org/10.1109/Transducers50396.2021.9495707

[8] Ng, D. K. T., Chen, W., Xu, L., Lau, H. J. E., Tobing, L. Y. M., Ho, C. P., Chung, W. W., Jaafar, N., Fu, H., Zhang, Q., "SF_6 mixed in N_2 gas sensing responses from CMOS compatible AlN and ScAlN pyroelectric detectors," Proc. SPIE 12899, MOEMS and Miniaturized Systems XXIII, 128990J (2024). https://doi.org/10.1117/12.3002138

[9] Whatmore, R. W., "Pyroelectric devices and materials," Rep. Prog. Phys., 49, 1335-1386 (1986). https://doi.org/10.1088/0034-4885/49/12/002

[10] Xu, L., Ng, D. K. T., Chen, W., Li, N., Ho, C. P., Goh, D. J., Zhang, Y., Zhang, Q., Lee, L. Y. T., "Low-power contactless button system based on MEMS ScAlN pyroelectric detector," Proc. SPIE 12434, MOEMS and Miniaturized Systems XXII, 1243405 (2023). https://doi.org/10.1117/12.2648806

[11] Ng, D. K. T., Chen, W., Wang, H., Gu, Z., Md Husni, Md H. K., Koh, I. J. W. Y., Xu, L., Wee, K. P. X., Ho, C. P., Goh, J. S., Zhang, Q., "Hydrogen Sensor (400 ppm – 1%) based on 20% ScAlN pyroelectric detector for a sustainable society," Proc. SPIE 12885, Terahertz, RF, Millimeter and Submillimeter-Wave Technology and Applications XVII, 128850Z (2024). https://doi.org/10.1117/12.3021874

[12] Ng, D. K. T., Ho, C. P., Zhang, T., Xu, L., Siow, L. Y., Chung, W. W., Cai, H., Lee, L. Y. T., Zhang, Q., Singh, N., "CMOS compatible MEMS pyroelectric infrared detectors: from AlN to ScAlN," Proc. SPIE 11697, MOEMS and Miniaturized Systems XX, 116970N (2021). https://doi.org/10.1117/12.2582707

[13] Ng, D. K. T., Wu, G., Zhang, T. –T., Xu, L., Sun, J., Chung, W. –W., Cai, H., Zhang, Q., Singh, N., "Considerations for an 8-inch wafer-level CMOS compatible AlN pyroelectric 5-14 µm wavelength IR detector towards miniature integrated photonics gas sensors," Journal of Microelectromechanical Systems, 29 (5), 1199-1207 (2020). https://doi.org/10.1109/JMEMS.2020.3015378

[14] Ng, D. K. T., Zhang, T., Siow, L. Y., Xu, L., Ho, C. P., Cai, H., Lee, L. Y. T., Zhang, Q., Singh, N., "A functional CMOS compatible MEMS pyroelectric detector using 12%-doped scandium aluminum nitride," Applied Physics Letters, 117, 183506 (2020). https://doi.org/10.1063/5.0024192

[15] Ranu, B, U., Sinha, R., Agarwal, P. B., "CMOS compatible pyroelectric materials for infrared detectors," Materials Science in Semiconductor Processing 140, 106375 (2022). https://doi.org/10.1016/j.mssp.2021.106375

[16] Kurz, N., Lu, Y., Kirste, L., Reusch, M., Žukauskaitė, A., Lebedev, V., Ambacher, O., "Temperature Dependence of the Pyroelectric Coefficient of AlScN Thin Films," Phys. Status Solidi A 215, 1700831 (2018). https://doi.org/10.1002/pssa.201700831

[17] Ng, D. K. T., Ho, C. P., Xu, L., Zhang, T., Siow, L. Y., Ng, E. J., Cai, H., Zhang, Q., Lee, L. Y. T., "CMOS-MEMS $Sc_{0.12}Al_{0.88}N$-based pyroelectric infrared detector with CO_2 gas sensing," 2021 IEEE 34th International Conference on Micro Electro Mechanical Systems (MEMS), Gainesville, FL, USA, 852-855, (2021). https://doi.org/10.1109/MEMS51782.2021.9375435

[18] Ng, D. K. T., Zhang, T., Siow, L. Y., Xu, L., Ho, C. P., Cai, H., Lee, L. Y. T., Zhang, Q., Singh, N., "Improved specific detectivity to 10^7 for CMOS-MEMS pyroelectric detector based on 12%-doped scandium aluminum nitride," 2021 IEEE 34th International Conference on Micro Electro Mechanical Systems (MEMS), Gainesville, FL, USA, 860-863, (2021). https://doi/org/10.1109/MEMS51782.2021.9375145

[19] Ruotsalainen, K., Morits, D., Ylivaara, O. M. E., Kyynäräinen, J., "Resonating AlN-thin film MEMS mirror with digital control," Journal of Optical Microsystems 2 (1), 011006 (2022). https://doi.org/10.1117/1.JOM.2.1.011006

[20] Tong, A. S. K., Chung, W. W., Goh, C., Tobing, L. Y. M., Lim, L. W., Akimov, Y. A., Quek, Z. J., Anthur, A. P., Goh, J. S., Lin, H., Singh, N., Zhang, Q., Ng, D. K. T., "1 Million Intrinsic Q-Factor Microring Resonators from PVD Aluminum Nitride on SiO_2-on-Si Substrate," 2024 Optical Fiber Communications Conference and Exhibition (OFC), San Diego, CA, USA, 2024, pp. 1-3. https://doi.org/10.1364/OFC.2024.Tu2B.4

[21] Ng, D. K. T., Xu, L., Fu, Y. H., Chen, W., Ho, C. P., Goh, J. S., Chung, W. W., Jaafar, N., Zhang, Q., Lee, L. Y. T., "CMOS AlN and ScAlN pyroelectric detectors with optical enhancement for detection of CO_2 and CH_4 gases," Adv. Electron. Mat. 9, 2300256 (2023). https://doi.org/10.1002/aelm.202300256

[22] Swinehart, D. F., "The Beer-Lambert Law," Journal of Chemical Education 39 (7), 333 (1962). https://doi.org/10.1021/ed039p333

[23] Dolan, J., "Chromatographic Measurements, Part 5: Determining LOD and LOQ Based on the Calibration Curve," Separation Science (9 Feb 2021). https://www.sepscience.com/hplc-solutions-126-chromatographic-measurements-part-5-determining-lod-and-loq-based-on-the-calibration-curve/